

Catalytic CavitanDs

Introverted Phosphorus-Au CavitanDs for Catalytic Use

Michael P. Schramm,^[a] Mao Kanaura,^[b] Kouhei Ito,^[b] Masataka Ide,^[b] and Tetsuo Iwasawa*^[b]

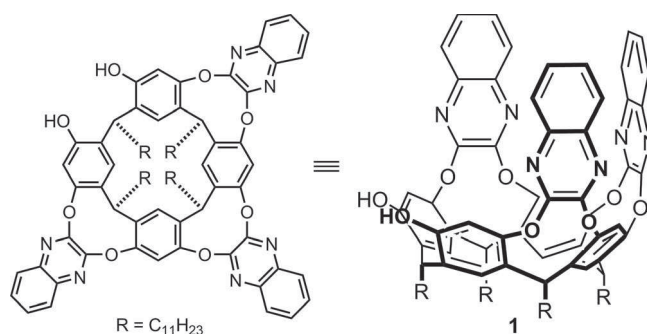
Abstract: A preparative synthesis of an inwardly directed phosphoramidite-Au complex is described and a description of some of its catalytic performance. The molecular structure was determined by crystallographic analysis, which disclosed that the phosphoramidite ligand points “out” and places the complexed

Au “in”. We investigated its catalytic activities and found that the inwardly directed Au is surrounded by three inert walls that provide new opportunities for supramolecular catalysis and study of reactive intermediates.

Introduction

Natural receptors like enzymes and RNA strands have their functional groups oriented inwards for molecular recognition.^[1,2] Amino acid functional groups converge to create reactive sites inside the hydrophobic pockets, and the grooves of nucleic acids are also concave and lined with convergent functionality to fold around guest substrates. Thus they serve as incredibly well-organized chemical catalysts to perform numerous biological operations.^[3] Inspired by these, organic chemists have developed artificial receptors that bear functional substituents inside chemical space.^[4–6] Such an inwardly directed “introverted” functional group is a form of synthetic receptor originally designed by Rebek, in which a reactive site converges onto a concave surface of resor[4]arene-based cavitand.^[7] The Rebek group has deployed these introverted functionalized cavitands as beautiful tools to understand facets of bio-relevant reactions;^[8–11] however, introverted functional groups have not developed into a powerful synthetic platform. Two shortcomings provide chemists a continuing challenge. The first problem is the synthetic difficulty to prepare even 100 mg of functionalized cavitands.^[12] The second is hardships in the synthesis of cavitand/organometal hybrids in which introverted functionality acts as a supporting ligand to make a complex with transition metals.^[13] Overcoming these two drawbacks perhaps will allow cavitands to make more significant inroads in the synthetic community, and a properly built hybrid may one day work as a real tool for new modes of chemical catalysis and discovery.^[14,15]

Recently, we have reported the synthesis of introverted functionality tethered to a cavitand scaffold of triquinoxaline-spanned resorcin[4]arene **1** (Scheme 1) with dialkylsilanes^[16] and allylsilanes.^[17] The introverted allyl cavitand enabled us to realize that it has higher reactivity than the extroverted one toward *meta*-chloroperoxybenzoic acid (mCPBA). Such a supramolecular effect drove us to develop a new pyridine *N*-oxide cavitand as a supporting ligand in transition metal catalyzed reactions,^[18] but *N*-oxide was unsuccessful in a variety of otherwise straightforward catalytic transformations. We thus have focused our attention on supramolecular frameworks that would support an inwardly located metal center for improving chemical transformations.



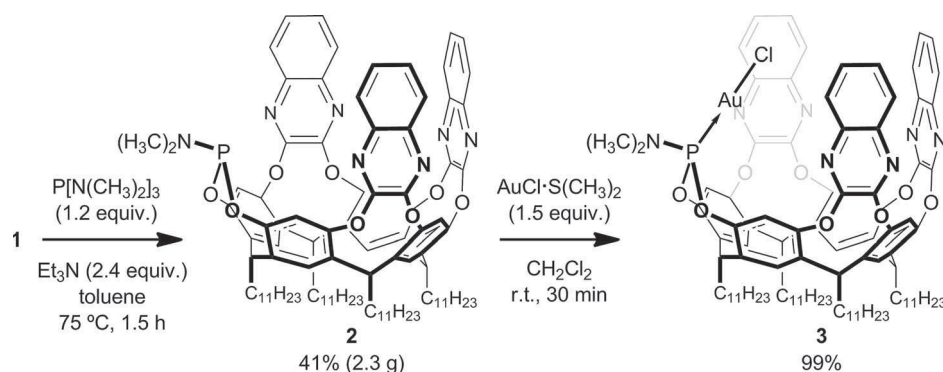
Scheme 1. Triquinoxaline-spanned resorcin[4]arene **1**.

Herein we report the preparative synthesis of hybrid complex **3**, the result of a simple reaction between phosphoramidite **2** and AuCl·S(CH₃)₂ (Scheme 2). Compound **2** was readily prepared (2.3 g scale) as one of two possible isomers (“in” or “out”) in one step from **1**. Upon reaction of **2** with AuCl·S(CH₃)₂, new complex **3** was prepared quantitatively. Its X-ray structural analysis unveiled the previously unconfirmed orientation of phosphoramidite moiety of **2**, and the ORTEP figure reveals the details of an inwardly directed Au that resides inside the cavity. Thus, bulky **2** was selectively installed in an outward position with its electrons pointing inward. The potential of this complex is significant; Au is located inward, flanked by three walls of “organized solvent”.

[a] Department of Chemistry and Biochemistry, California State University Long Beach (CSULB), 1250 Bellflower Blvd. Long Beach, Los Angeles, CA 90840, USA <https://schrammlab.wordpress.com/>

[b] Department of Materials Chemistry, Ryukoku University, Seta, Otsu, Shiga, 520-2194, Japan E-mail: iwasawa@rins.ryukoku.ac.jp <http://www.chem.ryukoku.ac.jp/iwasawa/index.html>

Supporting information for this article is available on the WWW under <http://dx.doi.org/10.1002/ejoc.201501426>.



Scheme 2. Preparative synthesis of introverted phosphoramidite **2** from **1**, and subsequent complexation with $\text{AuCl}\cdot\text{S}(\text{CH}_3)_2$ to give **3**.

Analogously, we synthesized two other phosphorus cavitands with variation to the external phosphorus substituent. Finally, we found that the Au–Cl complexes reported herein have catalytic activity consistent with Au^{I} ; addition of water to terminal alkynes and cyclization of diketo-alkynes occurs. These initial results set the stage to explore the consequences of a new inwardly directed Au^{I} catalytic center, surrounded by three solvent walls. The trapping of reactive intermediates and size exclusion of substrates and intermediate stabilization are tantalizing possibilities that drive this work.^[19]

Results and Discussion

Phosphorus **2** was reported in 2008 from our group.^[16] On a 0.1 mmol scale, 89 mg of **2** was isolated (57 % yield), the isomeric ratio was about 95:5.^[20,21] The stereochemical outcome was assumed to place the amine group outwards. By revisiting this reaction we could successfully isolate one major isomer on a 2.3-gram scale (short-plug, CH_2Cl_2). Reaction with $\text{AuCl}\cdot\text{S}(\text{CH}_3)_2$ gave quantitative formation of Au cavitand **3** (Scheme 2). The molecular structure of **3** was determined by crystallographic analysis, which disclosed the introverted Au arrangement (Figure 1).^[22] Several crystals were grown and, in the one reported, we find a molecule of CH_2Cl_2 in the interior, sandwiched between gold and the cavitand walls, see Figure 1 (a and b). The ^1H NMR spectrum of **3** showed a single conformer; for example, a dimethyl group of $-\text{PN}(\text{CH}_3)_2$ gave just one peak at 3.07 ppm (d, $^3J_{\text{PH}} = 12.9$ Hz, 6 H) in CDCl_3 .

In a similar fashion, methoxy phosphite 3-walled cavitand **4** was prepared from **1** by reaction with $\text{P}(\text{OCH}_3)_3$ (Scheme 3). Silica gel column chromatography was sufficient to isolate the two isomers that formed; outwardly directed **4a** was isolated in 57 % yield, and inward **4b** in 21 % yield. The methyl group of CH_3OP **4a** in CDCl_3 is located at $\delta = 3.92$ ppm (d, $^3J_{\text{PH}} = 8.3$ Hz), and in **4b** is shifted to upfield 2.99 ppm (d, $^3J_{\text{PH}} = 12.4$ Hz) due to the anisotropic effect of the π electron-clouded space.^[16] Subsequent complexation of **4a** with $\text{AuCl}\cdot\text{S}(\text{CH}_3)_2$ gave **5** in quantitative yield. We were unable to collect crystals of suitable quality for X-ray analysis, but from the in-out anisotropy observed in **4a** versus **4b** we have made confidently our stereochemical assignment of **5**.

In a final example, phenyl phosphonite **6** was prepared in 60 % isolated yield as a single isomer (as determined by NMR

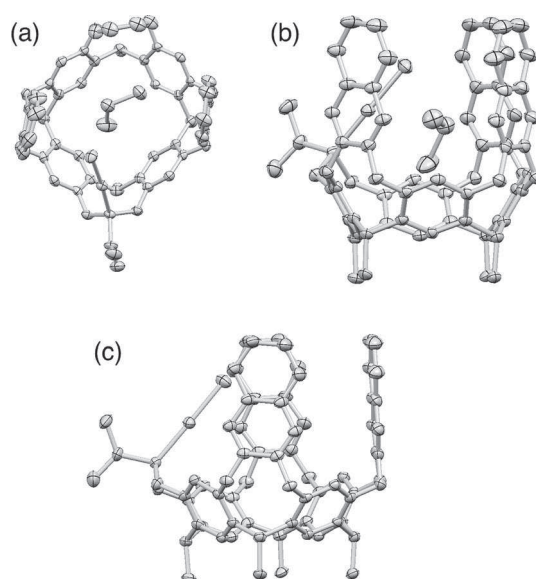
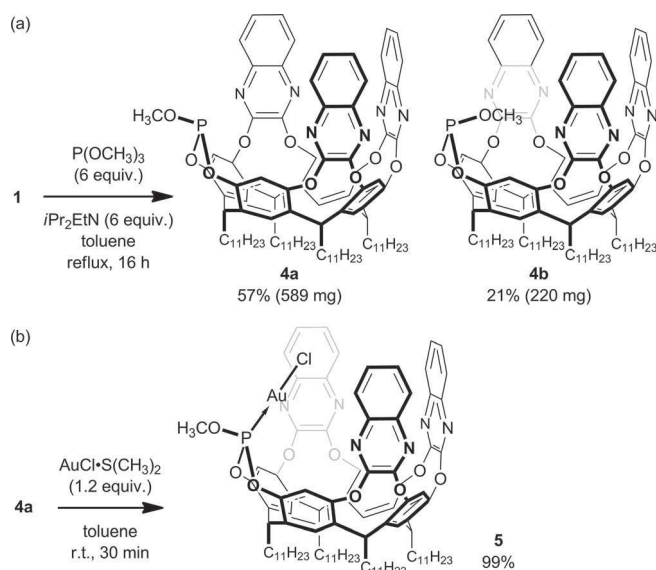
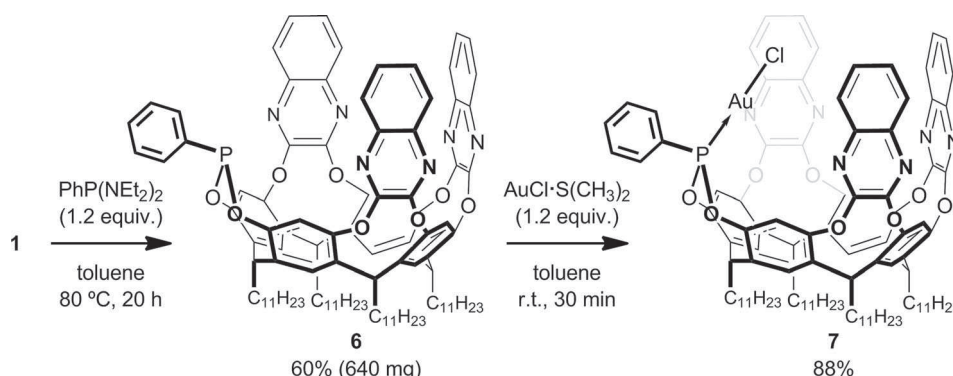


Figure 1. ORTEP drawing of **3**· CH_2Cl_2 with thermal ellipsoids at the 50% probability level; (a) top view; (b) side view; (c) side view of **3** with interior CH_2Cl_2 omitted for clarity. Hydrogen atoms are omitted for clarity. Selected bond lengths [Å]: P–Au 2.196, Au–Cl 2.303, P–N 1.622.



Scheme 3. (a) Synthesis of intro- and extroverted phosphite **4**; (b) complexation of **4a** with $\text{AuCl}\cdot\text{S}(\text{CH}_3)_2$ to give **5**.



Scheme 4. Selective synthesis of introverted phosphonite **6**, and subsequent complexation with $\text{AuCl}\cdot\text{S}(\text{CH}_3)_2$ to give **7**.

spectroscopy)^[21] from reaction of **1** with $\text{PhP}[\text{N}(\text{CH}_2\text{CH}_3)_2]_2$ (Scheme 4). The reaction of **6** and $\text{AuCl}\cdot\text{S}(\text{CH}_3)_2$ successfully gave complex **7** in 88 % yield. For complex **7** (and corresponding **6**) the chemical shifts of the phenyl group show no indication of upfield shifts and thus it is reasonable to assume that the group is outwardly directed, whereas Au is inwardly directed. The chemical shifts of the resorcin[4]arene bridging methines for **7** are consistent with those for **5** and **3**. From these results it appears that the larger size of dimethylamine (for **2**) or phenyl (for **6**) direct the stereochemical outcome of the reaction. The smaller methoxy (see **4a** and **4b**) afforded appreciable amounts of stereoisomers.

Before reporting on our catalytic results, we make the following observations about the solution dynamics of **3**. 4-Walled quinoxaline cavitands are known to fluctuate between vase (closed) and kite (open) conformations and reports on the effects of solvent and acid are known.^[23] Typically, methine protons around $\delta = 5.5$ ppm are indicative of vase conformers, whereas $\delta = 3.7$ ppm indicates the kite form. For **2** in Table 1, proton H^c is in a different electronic environment than the other two protons H^a and H^b . H^a and H^b in all solvents clearly demon-

strate the vase is preferred. Some variation exists and the differences observed between chlorinated to aromatic solvents are consistent with previous observations.^[23] For **3**, we see nearly identical behavior of the methines relative to parent **2**. No major perturbations to structure are observed and the molecule is well behaved with sharp methines; H^a and H^b protons are consistent in all solvents with a vase shape. The latter observation coupled with solid-state evidence supports the idea that the metal center is pointing inwardly in solution.

We next took **3** and examined it for catalytic activity. A variety of recent reviews on the subject of Au-catalyzed reactions exist.^[24] These served as inspiration for our initial screenings; hydration of terminal alkynes, and Conia-ene reaction of β -keto ester alkynes were adopted. For hydration of terminal alkynes, we attempted a simple hydration reaction by following reports with Au.^[25] We first began by mixing ethynylbenzene with **3** (Figure 2). After 24 h, the ^1H NMR spectrum showed that the alkyne and **3** were unreacted [Figure 2(b)]. Addition of AgOTf [Figure 2(c)] and waiting for 2 h nearly eliminated all traces of

Table 1. NMR chemical shifts of the methine protons H^a – H^c of **2** and **3**.

Solvent	H^a	H^b	H^c	$\text{H}^{a'}$	$\text{H}^{b'}$	$\text{H}^{c'}$
CD_2Cl_2	5.32	5.66	4.57	5.64	5.76	4.55
CDCl_3	5.68	5.68	4.54	5.70	5.76	4.53
$[\text{D}_6]$ benzene	6.10	6.20	5.13	6.07	6.18	4.75
$[\text{D}_8]$ toluene	6.04	6.12	5.02	6.05	6.09	4.74
$[\text{D}_{10}]$ - <i>p</i> -xylene	6.01	6.06	4.93	5.97	6.03	4.72
$[\text{D}_{12}]$ mesitylene	(5.82) ^[a]	–	–	(5.78) ^[a]	(5.54) ^[a]	–

[a] Peaks were broadened, but small averaged peaks could be observed.

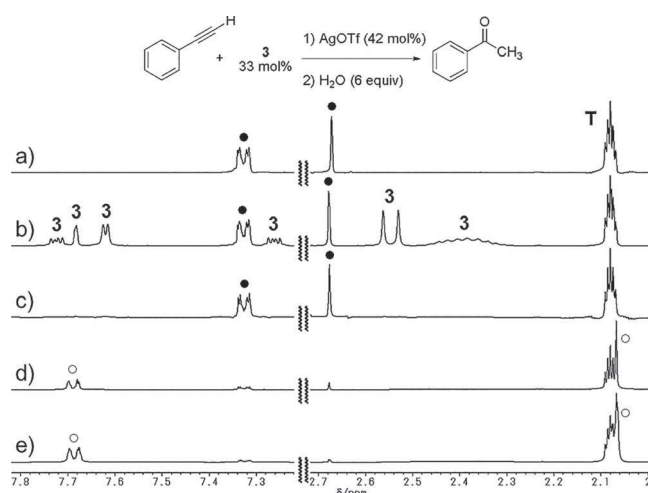


Figure 2. Up- and downfield portion of the ^1H NMR (400 MHz, $[\text{D}_8]$ toluene) spectra for (a) ethynylbenzene (0.019 mmol); (b) 33 mol-% **3** added and left at room temp. for 24 h; (c) 42 mol-% AgOTf added and left at room temp. for 2 h; (d) 6 equiv. of water added and heated to 85 °C for 1 h; and (e) heated for 40 h. Each resonance labeled with T, black circle, and white circle corresponds to residual C_7H_8 , ethynylbenzene, and acetophenone, respectively.

3 from the solution spectra. Small non-descript features remain, and a very slight trace of a new species emerges at $\delta \approx 7.68$ ppm. Next, an excess of water was added and the reaction was heated to 85 °C, after which the concentration of ethynylbenzene drastically decreased with a concomitant increase in the formation of benzophenone [Figure 2(d)].^[26,27] Continued heating for 40 h resulted in more hydration of alkyne to ketone [Figure 2(e)]. However, black metal residues were gradually observed; thus, the Au atom can leave the parent ligand and the Au complex might decompose.

To confirm the identity of the active species we changed the order of addition (Figure S1),^[28] ethynylbenzene was first mixed with AgOTf and no reaction was observed. Addition of water and heating also resulted in intact material. Finally the addition of 5 mol-% **3** with heating resulted in the formation of benzophenone. After an additional 12 h of heating there was low total conversion to benzophenone (12 %), with 83 % of starting alkyne remaining. At the time the reaction remained unoptimized but the results demonstrated the need of both Au and Ag species. Neither species catalyzes the reaction on its own and the observation in the disappearance of cavitand peaks when **3** was treated with AgOTf [Figure 2(b) versus (c)] supports an Au cationic species as being the active catalyst. Furthermore, HRMS (MALDI-TOF) of **3** gives three major ions in decreasing order of intensity: [**3** - Cl]⁺, [**3** + 2H]⁺, [**3** + Na]⁺. The major ion is from ready loss of "Cl" under ionizing conditions, which attests to the ease of Au⁺ formation. When **3** was mixed with an equal molar amount of AgOTf in CH₂Cl₂ for 15 min then analyzed by MS, no evidence of [**3**]⁺, [**3** + H]⁺ or [**3** + Na]⁺ species was observed, instead [**3** - Cl]⁺ was the only identifiable peak.^[29] Based on NMR and MS data, cationic Au formation by "**3** - Cl" is envisioned as the active catalyst species.

We optimized the conditions for the hydration of aromatic terminal alkynes by mixing 5 mol-% each of **3** and AgOTf and heating for 30 min, which resulted in an active catalyst species (Table 2). Upon addition of water and alkynes and heat for 1.5 h, we noted conversion under several conditions. Final measurements were made at 19 h. We find ethynylbenzene is converted slowly and in modest final yield of acetophenone (Table 2, Entries 1 and 2). By moving to the more bulky 1-ethynyl-naphthalene the results mimic those for ethynylbenzene (Table 2, Entry 3). When mesitylene was substituted as the solvent the results were disappointing (Table 2, Entry 4). This is interesting because mesitylene is widely reported to be too large to occupy the internal space. Indeed, NMR spectroscopic analysis in mesitylene of the cavitand species is difficult (Table 1). In this instance we expected toluene would compete for the catalytic site better and perhaps mesitylene would result in improved yields, but the opposite was true. We moved to 9-ethynylanthracene (Table 2, Entries 5 and 6),^[30] whereas the bulk of the substrate has increased drastically, so too has the reactivity of the alkyne.

Aromatic alkynes have two competing factors for reactivity with **3**, size and electronics. These factors for the three substrates are inversely related. Downfield shifts of the alkyne proton reveal information about the electronic character of the alkyne (in CDCl₃; ethynylbenzene-*H* δ = 3.07 ppm, 1-ethynyl-

Table 2. Results of the catalytic hydration of terminal aromatic alkynes.^[a]

$$\text{R}-\text{C}\equiv\text{C} \xrightarrow[\text{solvent, 85 }^\circ\text{C, overnight}]{\text{5 mol-\% } \mathbf{3}, \text{ 5 mol-\% AgX, H}_2\text{O (1 equiv.)}} \text{R}-\text{C}(=\text{O})-\text{CH}_3$$

Entry	R	X	Solvent	Conversion ^[b]	
				1.5 h	19 h
1	Ph	OTf	[D ₈]toluene	15 %	43 % ^[c]
2	Ph	OTf	[D ₁₂]mesitylene	14 %	49 %
3	1-naphthyl	OTf	[D ₈]toluene	4 %	48 % ^[c]
4	1-naphthyl	OTf	[D ₁₂]mesitylene	5 %	16 %
5	9-anthryl	OTf	[D ₈]toluene	81 % ^[c]	100 %
6	9-anthryl	OTf	[D ₁₂]mesitylene	54 %	98 %
7	Ph	SbF ₆	[D ₈]toluene	4 %	49 %
8	Ph	BF ₄	[D ₈]toluene	3 %	4 %

[a] Substrate (0.056 mmol), H₂O (0.056 mmol), **3** (5 mol-%), AgX (5 mol-%), and solvent (0.55 mL). [b] Conversion = integration of product protons divided by normalized total area of substrate and product. No other major peaks were observed. [c] Representative ¹H NMR spectrum is included in the Supporting Information.

naphthalene-*H* δ = 3.48 ppm, 9-ethynylanthracene-*H* δ = 4.00 ppm). The last species is unstable when stored.

Gold **3** shows more promise for aliphatic alkynes (Table 3). 1-Hexyne is completely converted into 2-hexanone in less than 1 h with heating (Table 3, Entry 1). The reaction in CDCl₃ was sluggish and incomplete (Table 3, Entry 2). Increasingly bulky alkynes, such as 4-phenyl-1-butyne and *tert*-butylacetylene, also showed good conversion (Table 3, Entries 3 and 4). These latter two alkynes had similar reactivity profiles to each other, and the reaction is only half complete after 1 h and requires 16 h to approach good conversion. With these results we predict future application of **3** may include size-selective reactivity. At this time, however, the cavitand does not have significant selective ability, but these studies are the beginning of our exploration.

Table 3. Results of the catalytic hydration reaction of terminal aliphatic alkynes.^[a]

$$\text{R}-\text{C}\equiv\text{C} \xrightarrow[\text{solvent, 85 }^\circ\text{C, overnight}]{\text{5 mol-\% } \mathbf{3}, \text{ 5 mol-\% AgOTf, H}_2\text{O (1 equiv.)}} \text{R}-\text{C}(=\text{O})-\text{CH}_3$$

Entry	R	Solvent	Conversion ^[b]		
			1 h	4 h	16 h
1	CH ₃ (CH ₂) ₃	[D ₈]toluene	100 %	–	–
2	CH ₃ (CH ₂) ₃	CDCl ₃ (65 °C)	25 %	26 %	29 %
3	Ph(CH ₂) ₂	[D ₈]toluene	52 %	72 %	79 %
4	(CH ₃) ₃ C	[D ₈]toluene	49 %	67 %	89 %

[a] Substrate (0.056 mmol), H₂O (0.056 mmol), **3** (5 mol-%), and solvent (0.55 mL). [b] Conversion = integration of product protons divided by normalized total area of substrate and product. No other major peaks were observed.

Next, we examined the ability of **3** to catalyze Conia-ene reactions (Table 4).^[31,32] We were inspired by this work as an entry point to test the substrate size, solvent effects of the cavitand scaffold, and the effect of the ligand in **3**, **5**, and **7**. Brief

heating of Au and Ag in deuterated solvent followed by subsequent treatment with **8** and further heating resulted in product formation. The catalytic conversion of **8** to **9** was easy to follow by NMR spectroscopy, with several chemically distinct protons. After 1 h of heating we identified **9** in 10 % conversion (Table 4, Entry 1), with 65 % of remaining **8**. The 25 % of material was **10** that resulted from direct hydration of the terminal alkyne. Despite not adding water, adventitious water appears to be incorporated into the triple bond. Compound **9** is known, and **10** was isolated and characterized by ^1H NMR spectroscopy (see Supporting Information). The reaction was allowed to heat and resulted in an equal distribution of **8**, **9**, and **10**. By changing solvent to CDCl_3 (Table 4, Entry 2) we found that after 1 h, **10** was the major new species formed, but at 17 h, 62 % of the total material was **9**. At this stage we decided to analyze the differences between **3**, **5**, and **7**. After initial studies, it appears there is an advantage to the use of the P–N **3**. Indeed P–Ph and P–OMe ligands left much of **8** unreacted after 17 h (Table 4, Entries 3 and 4). This result has not been fully explored, but it is easy to envision P–N provides an added degree of electron donation into the P center.

Table 4. Results of Conia-ene reactions of **8**.^[a]

Entry	Catalyst	Solvent (Temp.)	Time	8 ^[b]	9 ^[b]	10 ^[b]
1	3	[D ₈]toluene (85 °C)	1 h	65 %	10 %	25 %
			2.5 h	53 %	20 %	26 %
			17 h	35 %	34 %	33 %
2	3	CDCl_3 (60 °C)	1 h	69 %	3 %	20 %
			17 h	17 %	62 %	28 %
3	5	CDCl_3 (60 °C)	1 h	72 %	3 %	23 %
			17 h	55 %	23 %	25 %
4	7	CDCl_3 (60 °C)	1 h	75 %	2 %	23 %
			17 h	42 %	25 %	33 %

[a] Compound **8** (0.056 mmol), H_2O (0.056 mmol), and solvent (0.55 mL).

[b] Conversion = integration of product protons divided by normalized total area of substrate and product. No other major peaks were observed.

Conclusions

In summary, the arrangement of an Au atom, which points inward and is flanked by 3 aromatic walls, provides a new architecture for catalysis. This result differs from the first discoveries in the field^[10(a),14] in which the inwardly directed functionality was organic in nature and blocked access to the concave surface. A Pd-bound cavitand is known^[13] but has fewer proclivities for directing the metal center truly inward. The case of **3**, **5**, and **7** differs from these archetypes: the top of the catalytic site remains open so that guests can sample the space, enter and leave. Au cavitands are also less likely to be complicated by product inhibition, in which the product itself becomes the

best guest. Au plays a special role in this first instance; it has robust and important reactivity that can be tuned directly through the ligand set. There are many more variations of reactions to try. In these endeavors we look forward to reporting on supramolecular advantages of this easily accessed chemical platform.

Experimental Section

General Methods: All reactions sensitive to air or moisture were carried out under an argon atmosphere and anhydrous conditions. Dry solvents were purchased and used without further purification and dehydration. All reagents were used as received. Analytical thin layer chromatography was carried out on Merck silica 60F₂₅₄. Column chromatography was carried out with silica gel 60 N (Kanto Chemical Co.). HRMS were reported on the basis of TOF (time of flight), and EB (double-focusing) techniques. ^1H and ^{13}C , and ^{31}P NMR spectra were recorded with a 5 mm QNP probe at 400, 100, and 162 MHz, respectively. Chemical shifts are reported to residual solvent signals (^1H NMR: CHCl_3 δ = 7.26, C_7H_8 δ = 2.08, C_6H_6 δ = 7.16, CH_2Cl_2 δ = 5.32; ^{13}C NMR: CDCl_3 δ = 77.0). Signal patterns are indicated as s for singlet, d for doublet, t for triplet, q for quartet, m for multiplet, br. for broad.

Gram-Scale Synthesis of Phosphoramidite 2: (see Scheme 2) Under an N_2 atmosphere, to a three-necked 300 mL flask charged with triquinoline-spanned resorcin[4]arene **1**– (5.34 g, 3.6 mmol) and dry toluene (72 mL) in a pre-heated 75 °C oil bath was added Et_3N (1.2 mL, 8.6 mmol). Then, tris(dimethylamino)phosphine (0.77 mL, 4.3 mmol) was added. After stirring for 1.5 h, complete consumption of the starting resorcin[4]arene was ensured by TLC monitoring and the reaction mixture was cooled to ambient temperature. The mixture was filtered through a pad of Celite, and the filtrate was concentrated in vacuo to give 5.82 g of yellow solid compounds. Purification by short-plug column chromatography (CH_2Cl_2) afforded 2.64 g of **2** in 41 % yield as a white solid. ^1H NMR (400 MHz, CDCl_3): δ = 8.31 (s, 2 H), 8.01 (d, J = 8.3 Hz, 2 H), 7.74–7.70 (m, 4 H), 7.59 (dd, J = 8.3, 8.3 Hz, 2 H), 7.49 (dd, J = 8.3, 8.3 Hz, 2 H), 7.39 (dd, J = 6.1, 3.3 Hz, 2 H), 7.23 (s, 2 H), 7.21 (s, 2 H), 7.19 (s, 2 H), 5.68 (t, J = 8.2 Hz, 3 H), 4.54 (t, J = 7.7 Hz, 1 H), 2.78 (d, $^3J_{\text{PH}}$ = 10.7 Hz, 6 H), 2.27–2.18 (m, 8 H), 1.58–1.28 (m, 72 H), 0.90–0.87 (m, 12 H) ppm. ^1H NMR (400 MHz, CD_2Cl_2): δ = 8.24 (s, 2 H), 7.97 (d, J = 7.7 Hz, 2 H), 7.76–7.73 (m, 4 H), 7.63 (dd, J = 7.7, 7.7 Hz, 2 H), 7.54 (dd, J = 7.7, 7.7 Hz, 2 H), 7.47 (dd, J = 6.2, 3.4 Hz, 2 H), 7.31 (s, 2 H), 7.26 (s, 2 H), 7.19 (s, 2 H), 5.67–5.64 (m, 3 H), 4.57 (t, J = 8.6 Hz, 1 H), 2.78 (d, $^3J_{\text{PH}}$ = 10.5 Hz, 6 H), 2.32–2.22 (m, 8 H), 1.47–1.29 (m, 72 H), 0.91–0.88 (m, 12 H) ppm. ^1H NMR (400 MHz, [D₈]toluene): δ = 8.69 (s, 2 H), 7.84 (dd, J = 5.9, 3.7 Hz, 2 H), 7.71–7.69 (m, 2 H), 7.69 (s, 2 H), 7.64 (s, 2 H), 7.61 (s, 2 H), 7.39 (d, J = 8.2 Hz, 2 H), 7.20 (dd, J = 5.9, 3.7 Hz, 2 H), 7.09–7.00 (m, 4 H), 6.12 (t, J = 8.1 Hz, 1 H), 6.04 (t, J = 8.1 Hz, 2 H), 5.01 (t, J = 7.7 Hz, 1 H), 2.54 (d, $^3J_{\text{PH}}$ = 10.2 Hz, 6 H), 2.50–2.41 (m, 8 H), 1.33–1.31 (m, 72 H), 0.96–0.93 (m, 12 H) ppm. ^{13}C NMR (100 MHz, CDCl_3): δ = 153.1, 153.0, 152.9, 152.7, 152.5, 152.2, 149.5 (d, J_{CP} = 4.8 Hz), 139.92, 139.89, 139.8, 137.1, 136.3, 136.0, 134.4, 129.3, 129.0, 128.8, 128.03, 128.00, 127.9, 123.5, 122.5, 119.1, 117.3, 35.8, 35.2 (d, J_{CP} = 18.2 Hz), 34.3, 34.2, 33.0, 32.1 (peaks overlap), 31.7, 29.9 (peaks overlap), 29.6 (peaks overlap), 28.2, 28.1, 22.9 (peaks overlap), 14.3 (peaks overlap) ppm. ^{31}P NMR (162 MHz, CDCl_3): δ = 141.0 ppm. ^{31}P NMR (162 MHz, CD_2Cl_2): δ = 141.0 ppm. ^{31}P NMR (162 MHz, [D₈]toluene): δ = 138.7 ppm. MS (ESI): m/z = 1591 [M + Cl][–]. $\text{C}_{98}\text{H}_{122}\text{N}_7\text{O}_8\text{P}$ (1557.06): calcd. C 75.60, H 7.90, N 6.30; found C 75.38, H 7.86, N 6.34.

Au Complex 3: (see Scheme 2) Under an N₂ atmosphere, to a solution of **2** (156 mg, 0.1 mmol) in anhydrous CH₂Cl₂ (3 mL) at ambient temperature was added AuCl-S(CH₃)₂ (44 mg, 0.15 mmol). After stirring for 30 min, **1** had been consumed (TLC monitoring). The reaction mixture was concentrated in vacuo to give a crude product in 196 mg as a white solid. Purification by short-plug column chromatography yielded 177 mg of **3** in 99 % as a white solid. ¹H NMR (400 MHz, CDCl₃): δ = 8.12 (s, 2 H), 7.85 (d, *J* = 8.1 Hz, 2 H), 7.80 (d, *J* = 8.1 Hz, 2 H), 7.76 (dd, *J* = 6.1, 3.4 Hz, 2 H), 7.53–7.45 (m, 6 H), 7.39 (s, 2 H), 7.26 (s, 2 H), 7.25 (s, 2 H), 5.76 (t, *J* = 8.4 Hz, 1 H), 5.70 (t, *J* = 8.1 Hz, 2 H), 4.54 (t, *J* = 8.1 Hz, 1 H), 3.09 (d, *J*_{PH} = 13.0 Hz, 6 H), 2.33–2.30 (m, 8 H), 1.45–1.28 (m, 72 H), 0.90–0.87 (m, 12 H) ppm. ¹H NMR (400 MHz, CD₂Cl₂): δ = 8.18 (s, 2 H), 7.96 (dd, *J* = 6.4, 3.4 Hz, 2 H), 7.74–7.72 (m, 4 H), 7.66 (dd, *J* = 6.4, 3.4 Hz, 2 H), 7.51–7.44 (m, 4 H), 7.36 (s, 2 H), 7.29 (s, 2 H), 7.27 (s, 2 H), 5.75 (t, *J* = 8.3 Hz, 1 H), 5.63 (t, *J* = 8.1 Hz, 2 H), 4.55 (t, *J* = 8.3 Hz, 1 H), 3.07 (d, ³*J*_{PH} = 12.9 Hz, 6 H), 2.35–2.01 (m, 8 H), 1.45–1.30 (m, 72 H), 0.91–0.88 (m, 12 H) ppm. ¹H NMR (400 MHz, C₆D₆): δ = 8.73 (s, 2 H), 8.03–8.00 (m, 4 H), 7.76 (s, 2 H), 7.71 (d, *J* = 8.4 Hz, 2 H), 7.65 (s, 2 H), 7.64 (s, 2 H), 7.32 (ddd, *J* = 6.2, 3.5 Hz, 2 H), 7.11 (ddd, *J* = 8.4, 7.0, 1.3 Hz, 2 H), 7.00 (ddd, *J* = 8.4, 7.0, 1.3 Hz, 2 H), 6.18 (t, *J* = 8.2 Hz, 1 H), 6.07 (t, *J* = 8.1 Hz, 2 H), 4.75 (t, *J* = 8.2 Hz, 1 H), 2.48 (d, ³*J*_{PH} = 12.9 Hz, 6 H), 2.43–2.36 (m, 8 H), 1.55–1.34 (m, 72 H), 0.96–0.93 (m, 12 H) ppm. ¹H NMR (400 MHz, [D₈]toluene): δ = 8.54 (s, 2 H), 7.94–7.90 (m, 4 H), 7.74–7.71 (m, 2 H), 7.69–7.68 (m, 2 H), 7.63 (s, 2 H), 7.62 (s, 2 H), 7.27 (dd, *J* = 6.4, 3.6 Hz, 2 H), 7.13 (dd, *J* = 6.4, 3.6 Hz, 4 H), 6.09 (t, *J* = 8.1 Hz, 1 H), 6.02 (t, *J* = 8.0 Hz, 2 H), 4.76–4.73 (m, 1 H), 2.55 (d, ³*J*_{PH} = 12.9 Hz, 6 H), 2.43–2.36 (m, 8 H), 1.45–1.31 (m, 72 H), 0.96–0.92 (m, 12 H) ppm. ¹³C NMR (100 MHz, CD₂Cl₂): δ = 153.2 (d, *J*_{CP} = 2.5 Hz), 153.1, 153.0, 152.8, 152.6, 152.3, 146.2 (d, *J*_{CP} = 4.1 Hz), 140.4, 140.0, 139.9, 137.0 (d, *J*_{CP} = 2.1 Hz), 136.53, 136.49 (d, *J*_{CP} = 3.1 Hz), 135.8, 129.9, 129.8, 129.5, 129.3, 128.2, 127.7, 124.4, 123.2, 118.8, 118.4 (d, *J*_{CP} = 4.1 Hz), 36.9 (d, *J*_{CP} = 11.5 Hz), 36.1, 34.8, 34.6, 33.2, 32.43, 32.42, 32.41, 30.5, 30.2 (peaks overlap), 30.0, 29.9 (peaks overlap), 28.6, 28.4, 28.3, 23.2 (peaks overlap), 14.4 (peaks overlap) ppm. ³¹P NMR (162 MHz, CD₂Cl₂): δ = 115.1 ppm. ³¹P NMR (162 MHz, [D₈]toluene): δ = 113.0 ppm. MS (MALDI-TOF): *m/z* = 1753 [M – Cl]⁺. IR (neat): ν̄ = 2921, 2851, 1480, 1399, 1330, 1268, 1146, 756 cm⁻¹. HRMS (MALDI-TOF): calcd. for C₉₈H₁₂₂AuClN₇O₈PNa 1810.8339 [M + Na]⁺; found 1810.8268.

Phosphite 4a and 4b: (see Scheme 3, a) Under an N₂ atmosphere, a flask charged with **1** (1.0 g, 0.67 mmol) and dry toluene (13 mL) was dipped into a pre-heated oil bath (135 °C). To the mixture were added *i*Pr₂EtN (0.71 mL, 4.1 mmol) and P(OCH₃)₃ (0.48 mL, 4.1 mmol). After stirring for 16 h, the reaction mixture was cooled to room temperature, and concentrated in vacuo to give 1.07 g of crude products. Purification by column chromatography (hexane/EtOAc/CH₂Cl₂ = 18:1:1) yielded 589 mg of white solids **4a** in 57 % yield and 220 mg of white solids **4b** in 21 % yield. For **4a**. ¹H NMR (400 MHz, CDCl₃): δ = 8.31 (s, 2 H), 7.98 (d, *J* = 8.3 Hz, 2 H), 7.75 (dd, *J* = 6.2, 3.4 Hz, 2 H), 7.73 (d, *J* = 8.3 Hz, 2 H), 7.58 (dd, *J* = 8.3, 8.3 Hz, 2 H), 7.48 (dd, *J* = 8.3, 8.3 Hz, 2 H), 7.43 (dd, *J* = 6.2, 3.4 Hz, 2 H), 7.29 (s, 2 H), 7.21 (s, 4 H), 5.70 (t, *J* = 8.1 Hz, 1 H), 5.70 (t, *J* = 8.1 Hz, 2 H), 4.52 (t, *J* = 7.2 Hz, 1 H), 3.92 (d, ³*J*_{PH} = 8.3 Hz, 3 H), 2.27–2.19 (m, 8 H), 1.42–1.28 (m, 72 H), 0.90–0.87 (m, 12 H) ppm. ¹H NMR (400 MHz, [D₈]toluene): δ = 8.67 (s, 2 H), 7.81–7.78 (m, 2 H), 7.72–7.70 (m, 2 H), 7.67 (s, 2 H), 7.64 (s, 4 H), 7.40–7.38 (m, 2 H), 7.20–7.17 (m, 2 H), 7.08–6.96 (m, 4 H), 6.11 (t, *J* = 8.0 Hz, 1 H), 6.04 (t, *J* = 8.1 Hz, 2 H), 4.90 (t, *J* = 7.8 Hz, 1 H), 3.65 (d, ³*J*_{PH} = 7.8 Hz, 3 H), 2.42–2.40 (m, 8 H), 1.47–1.30 (m, 72 H), 0.96–0.93 (m, 12 H) ppm. ¹³C NMR (100 MHz, CDCl₃): δ = 153.2 (two peaks overlap), 153.0, 152.9, 152.8, 152.7 (d, *J*_{CP} = 0.95 Hz), 147.2 (d, *J*_{CP} = 5.2 Hz), 140.11, 140.09 (two peaks overlap), 137.4 (d, *J*_{CP} = 2.2 Hz), 136.4, 136.3,

135.4, 129.6, 129.4, 129.2, 128.6, 128.2, 128.1, 123.7, 123.0, 119.4, 117.8, 50.4 (d, *J*_{CP} = 4.1 Hz), 36.1, 34.5, 34.4, 33.1, 32.3 (peaks overlap), 32.0, 30.1 (peaks overlap), 29.7 (peaks overlap), 28.4 (peaks overlap), 23.1 (peaks overlap), 14.5 (peaks overlap) ppm. ³¹P NMR (162 MHz, CDCl₃): δ = 127.2 ppm. ³¹P NMR (162 MHz, [D₈]toluene): δ = 125.1 ppm. IR (neat): ν̄ = 2921, 2851, 1605, 1578, 1482, 1400, 1332, 1273, 1157, 1029, 895, 757 cm⁻¹. MS (MALDI-TOF): *m/z* = 1544 ([M + H]⁺). HRMS (MALDI-TOF): calcd. for C₉₇H₁₂₀N₆O₉P 1543.8849 [M + H]⁺; found 1543.8983. C₉₇H₁₁₉N₆O₉P (1544.02): calcd. C 75.46, H 7.77, N 5.44; found C 75.26, H 7.69, N 5.27. For **4b**. ¹H NMR (400 MHz, CDCl₃): δ = 8.28 (s, 2 H), 7.98 (d, *J* = 8.2 Hz, 2 H), 7.77 (dd, *J* = 6.2, 3.5 Hz, 2 H), 7.62 (d, *J* = 8.2 Hz, 2 H), 7.57 (dd, *J* = 8.2, 8.2 Hz, 2 H), 7.49–7.43 (m, 4 H), 7.22 (s, 2 H), 7.18 (s, 2 H), 7.15 (s, 2 H), 5.72 (t, *J* = 8.0 Hz, 1 H), 5.66 (t, *J* = 8.2 Hz, 2 H), 4.47 (t, *J* = 7.9 Hz, 1 H), 2.99 (d, ³*J*_{PH} = 12.4 Hz, 3 H), 2.27–2.20 (m, 8 H), 1.43–1.28 (m, 72 H), 0.90–0.87 (m, 12 H) ppm. ¹³C NMR (100 MHz, CDCl₃): δ = 153.3, 153.2, 153.1, 153.0, 152.9, 152.2 (d, *J*_{CP} = 1.4 Hz), 148.7 (d, *J*_{CP} = 15.1 Hz), 140.14, 140.13, 140.09, 136.4, 135.4 (d, *J*_{CP} = 1.2 Hz), 134.8, 129.7, 129.3, 129.2, 128.3, 128.2, 127.8, 124.1, 122.5, 119.2, 117.4, 51.7 (d, *J*_{CP} = 22.2 Hz), 36.8, 34.5, 34.4, 33.1, 32.5, 32.3 (peaks overlap), 31.5, 30.1 (peaks overlap), 29.8, 28.41, 28.35, 28.3, 23.1 (peaks overlap), 14.5 (peaks overlap) ppm. ³¹P NMR (162 MHz, CDCl₃): δ = 110.6 ppm. IR (neat): ν̄ = 2921, 2851, 1578, 1481, 1399, 1331, 1267, 1158, 1016, 894, 757 cm⁻¹. MS (MALDI-TOF): *m/z* = 1544 [M + H]⁺. HRMS (MALDI-TOF): calcd. for C₉₇H₁₂₀N₆O₉P 1543.8849 [M + H]⁺; found 1543.8735. C₉₇H₁₁₉N₆O₉P (1544.02): calcd. C 75.46, H 7.77, N 5.44; found C 75.56, H 7.46, N 5.36.

Au Complex 5: (see Scheme 3, b) Under an N₂ atmosphere, to a solution of **4a** (118 mg, 0.078 mmol) in anhydrous toluene (1.5 mL) at ambient temperature was added AuCl-S(CH₃)₂ (28 mg, 0.094 mmol). After stirring for 30 min, **4a** was consumed (TLC monitoring). The reaction mixture was concentrated in vacuo to give 161 mg of crude product as a white solid compound. Purification by short-plug column chromatography (hexane/EtOAc = 4:1) yielded 137 mg of **5** in 99 % as a white solid. ¹H NMR (400 MHz, CDCl₃): δ = 8.17 (s, 2 H), 7.85 (dd, *J* = 8.0, 1.5 Hz, 2 H), 7.79–7.76 (m, 4 H), 7.54–7.44 (m, 8 H), 7.29 (s, 2 H), 7.25 (s, 2 H), 5.77 (t, *J* = 8.3 Hz, 1 H), 5.72 (t, *J* = 8.1 Hz, 2 H), 4.52 (t, *J* = 8.0 Hz, 1 H), 4.13 (d, ³*J*_{PH} = 13.6 Hz, 3 H), 2.33–2.18 (m, 8 H), 1.45–1.28 (m, 72 H), 0.91–0.87 (m, 12 H) ppm. ¹H NMR (400 MHz, [D₈]toluene): δ = 8.58 (s, 2 H), 7.93–7.88 (m, 4 H), 7.76–7.74 (m, 2 H), 7.66 (s, 2 H), 7.60 (s, 2 H), 7.57 (s, 2 H), 7.27–7.25 (m, 2 H), 7.13–7.11 (m, 4 H), 6.06 (t, *J* = 8.0 Hz, 1 H), 6.02 (t, *J* = 7.7 Hz, 2 H), 4.64 (t, *J* = 7.7 Hz, 1 H), 3.34 (d, ³*J*_{PH} = 14.4 Hz, 3 H), 2.40–2.33 (m, 8 H), 1.43–1.31 (m, 72 H), 0.94–0.91 (m, 12 H) ppm. ¹³C NMR (100 MHz, CDCl₃): δ = 153.2 (two peaks overlap), 152.9, 152.8, 152.5, 152.3, 143.9, 140.3, 140.2, 140.1, 138.2, 136.7, 136.0, 135.5, 129.9, 129.8, 129.5, 128.8, 128.1, 127.7, 124.0, 122.9, 119.3, 118.0 (d, *J*_{CP} = 4.1 Hz), 55.1, 36.0, 34.4, 33.0, 32.9, 32.3 (peaks overlap), 30.8, 30.1 (peaks overlap), 29.8 (peaks overlap), 28.4, 28.3, 28.2, 23.1 (peaks overlap), 14.5 (peaks overlap) ppm. ³¹P NMR (162 MHz, CDCl₃): δ = 108.5 ppm. ³¹P NMR (162 MHz, [D₈]toluene): δ = 111.0 ppm. IR (neat): ν̄ = 2921, 2851, 1480, 1398, 1329, 1155 cm⁻¹. MS (MALDI-TOF): *m/z* = 1740 [M – Cl]⁺. HRMS (MALDI-TOF): calcd. for C₉₇H₁₁₉AuClN₆O₉PNa 1797.8022 [M + Na]⁺; found 1797.7964.

Phophonite 6: (see Scheme 4) Under an N₂ atmosphere, a flask charged with **1** (1.0 g, 0.67 mmol) and dry toluene (13 mL) was dipped into a pre-heated oil bath (80 °C). To the mixture was added PhP(NEt₂)₂ (0.21 mL, 0.81 mmol). After stirring for 20 h, the reaction mixture was cooled to room temperature, and concentrated in vacuo to give 1.21 g of crude products. Purification by column chromatography (hexane) and precipitation (CH₂Cl₂/CH₃OH = 1:8) yielded 640 mg of white solids **6** in 60 %. ¹H NMR (400 MHz, CDCl₃):

δ = 8.34 (s, 2 H), 8.02 (d, J = 8.4 Hz, 2 H), 7.85–7.81 (m, 2 H), 7.74–7.72 (m, 4 H), 7.60 (dd, J = 7.0, 7.0 Hz, 2 H), 7.57–7.56 (m, 3 H), 7.48 (dd, J = 7.0, 7.0 Hz, 2 H), 7.40 (dd, J = 6.2, 3.4 Hz, 2 H), 7.31 (s, 2 H), 7.27 (s, 2 H), 7.25 (s, 2 H), 5.73 (t, J = 7.9 Hz, 2 H), 5.71 (t, J = 7.4 Hz, 1 H), 4.60 (t, J = 7.6 Hz, 1 H), 2.32–2.20 (m, 8 H), 1.47–1.27 (m, 72 H), 0.91–0.87 (m, 12 H) ppm. ^1H NMR (400 MHz, $[\text{D}_8]$ toluene): δ = 8.70 (s, 2 H), 7.83 (dd, J = 6.4, 3.5 Hz, 2 H), 7.75–7.63 (m, 9 H), 7.46 (d, J = 7.7 Hz, 2 H), 7.20 (dd, J = 6.4, 3.5 Hz, 2 H), 7.10–7.09 (m, 6 H), 7.01–6.97 (m, 2 H), 6.13–6.06 (m, 3 H), 5.01 (t, J = 7.7 Hz, 1 H), 2.44–2.38 (m, 8 H), 1.48–1.32 (m, 72 H), 0.96–0.92 (m, 12 H) ppm. ^{13}C NMR (100 MHz, CDCl_3): δ = 153.30, 153.25, 153.1, 152.9, 152.8, 152.6, 152.4 (d, J_{CP} = 3.8 Hz), 140.1 (two peaks overlap), 137.0 (d, J_{CP} = 3.1 Hz), 136.4, 136.3, 135.4, 131.7, 130.0, 129.8, 129.6, 129.3 (d, J_{CP} = 3.3 Hz), 129.1, 128.9 (d, J_{CP} = 6.2 Hz), 128.6, 128.3 (d, J_{CP} = 5.2 Hz), 128.1, 125.6, 123.6, 123.3, 119.4 (d, J_{CP} = 5.2 Hz), 117.1 (d, J_{CP} = 1.4 Hz), 36.2, 34.5, 34.4, 33.2, 32.3 (peaks overlap), 30.1 (peaks overlap), 29.8 (peaks overlap), 28.42, 28.37, 23.1, 14.5 (peaks overlap) ppm. ^{31}P NMR (162 MHz, CDCl_3): δ = 166.7 ppm. ^{31}P NMR (162 MHz, $[\text{D}_8]$ toluene): δ = 166.0 ppm. IR (neat): $\tilde{\nu}$ = 2921, 2850, 1572, 1480, 1400, 1331, 1268, 1158, 893, 758 cm^{-1} . MS (MALDI-TOF): m/z = 1590 $[\text{M} + \text{H}]^+$. HRMS (MALDI-TOF): calcd. for $\text{C}_{102}\text{H}_{122}\text{N}_6\text{O}_8\text{P}$ 1589.9056 $[\text{M} + \text{H}]^+$; found 1589.8893. $\text{C}_{102}\text{H}_{121}\text{N}_6\text{O}_8\text{P}$ (1590.09): calcd. C 77.05, H 7.67, N 5.29; found C 77.26, H 7.55, N 5.32.

Au Complex 7: (see Scheme 4) Under an N_2 atmosphere, to a solution of **6** (195 mg, 0.12 mmol) in anhydrous toluene (3 mL) at ambient temperature was added $\text{AuCl}_5(\text{CH}_3)_2$ (43 mg, 0.15 mmol). After stirring for 30 min, **6** was consumed (TLC monitoring). The reaction mixture was concentrated in vacuo to give 234 mg of crude white solid compounds. Purification by short-plug column chromatography (hexane/EtOAc/ CH_2Cl_2 = 8:1:1) yielded 197 mg of **7** in 88 % as a white solid. ^1H NMR (400 MHz, CDCl_3): δ = 8.19 (s, 2 H), 8.15 (dd, J = 7.2, 7.2 Hz, 2 H), 7.86 (d, J = 7.8 Hz, 2 H), 7.81–7.77 (m, 4 H), 7.73 (dd, J = 7.2, 7.2 Hz, 1 H), 7.67 (dd, J = 7.8, 3.4 Hz, 2 H), 7.53–7.45 (m, 8 H), 7.33 (s, 2 H), 7.29 (s, 2 H), 5.79 (t, J = 8.2 Hz, 1 H), 5.73 (t, J = 8.0 Hz, 2 H), 4.68 (t, J = 8.2 Hz, 1 H), 2.33–2.24 (m, 8 H), 1.45–1.28 (m, 72 H), 0.90–0.87 (m, 12 H) ppm. ^1H NMR (400 MHz, $[\text{D}_8]$ toluene): δ = 8.61 (s, 2 H), 7.98 (dd, J = 6.8, 3.5 Hz, 2 H), 7.91 (dd, J = 6.3, 3.4 Hz, 2 H), 7.81–7.77 (m, 4 H), 7.76 (s, 2 H), 7.66 (s, 2 H), 7.62 (s, 2 H), 7.27 (dd, J = 6.3, 3.4 Hz, 2 H), 7.15–7.05 (m, 7 H), 6.10–6.04 (m, 3 H), 4.80 (t, J = 7.8 Hz, 1 H), 2.43–2.38 (m, 8 H), 1.45–1.29 (m, 72 H), 1.00–0.91 (m, 12 H) ppm. ^{13}C NMR (100 MHz, CDCl_3): δ = 153.2 (d, J_{CP} = 2.2 Hz), 153.1, 153.0, 152.8, 152.5, 152.3, 140.3, 140.2, 140.1, 138.0 (d, J_{CP} = 2.2 Hz), 136.7, 136.1 (d, J_{CP} = 2.9 Hz), 135.5, 134.6, 132.8, 131.8, 131.6, 131.4, 129.8 (d, J_{CP} = 11.5 Hz), 129.5 (d, J_{CP} = 5.5 Hz), 129.4, 128.9, 128.1, 127.7, 124.0, 122.8, 119.2, 117.6 (d, J_{CP} = 4.3 Hz), 36.1, 34.4, 33.0, 32.3 (peaks overlap), 30.9, 30.1 (peaks overlap), 29.8 (peaks overlap), 28.4, 28.3 (peaks overlap), 23.0 (peaks overlap), 14.5 (peaks overlap) ppm. ^{31}P NMR (162 MHz, CDCl_3): δ = 131.7 ppm. IR (neat): $\tilde{\nu}$ = 2921, 2851, 1605, 1579, 1480, 1413, 1399, 1156, 909, 756 cm^{-1} . MS (MALDI-TOF): m/z = 1844 $[\text{M} + \text{Na}]^+$. HRMS (MALDI-TOF): calcd. for $\text{C}_{102}\text{H}_{121}\text{AuCl}_6\text{O}_8\text{PNa}$ 1843.8230 $[\text{M} + \text{Na}]^+$; found 1843.8217.

Tricarbonyl Compound 10: (see Table 4) This compound was isolated from Conia-ene reaction of keto ester alkyne **8** under the general reaction conditions after 16 h of heating with dichloroethane as the solvent and with 30.7 mg (0.156 mmol) of substrate. The reaction mixture was concentrated and purified by column chromatography in 2:1 hexane/EtOAc to give 4.5 mg (14 % isolated yield).

^1H NMR (400 MHz, CDCl_3): δ = 3.73 (s, 3 H), 3.40–3.44 (t, J = 7.6 Hz, 1 H), 2.40–2.44 (t, J = 7.2 Hz, 2 H), 2.22 (s, 3 H), 2.12 (s, 3 H), 1.80–1.87 (m, 2 H), 1.54–1.62 (m, 2 H), 1.22–1.30 (m, 2 H) ppm.

Supporting Information (see footnote on the first page of this article): The ^1H NMR and ^{13}C NMR spectra of all new compounds.

Acknowledgments

The authors thank the Japan Society of the Promotion of Science for an Invitational Fellowship (L-15528, long-term support to M. P. S.). Dr. Toshiyuki Iwai, Dr. Takatoshi Ito, and Dr. Seiji Watase at OMTRI are gratefully thanked for assistance with HRMS and crystallographic analyses.

Keywords: Synthetic methods · Homogeneous catalysis · Supramolecular chemistry · Cavitands · Introverted functionality

- [1] a) J. A. Gerlt, *Chem. Rev.* **1987**, *87*, 1079–1105; b) J. C. M. van Hest, D. A. Tirrel, *Chem. Commun.* **2001**, 1897–1904; c) M. V. Rodnina, W. Wintermeyer, *Curr. Opin. Struct. Biol.* **2003**, *13*, 334–340; d) K. Shen, A. C. Hines, D. Schwarzer, K. A. Pickin, P. A. Cole, *Biochim. Biophys. Acta Proteins Proteomics* **2005**, *1754*, 65–78.
- [2] a) G. Varani, *Annu. Rev. Biophys. Biomol. Struct.* **1995**, *24*, 379–404; b) V. J. DeRose, *Curr. Opin. Struct. Biol.* **2003**, *13*, 317–324; c) S. Shuman, C. D. Lima, *Curr. Opin. Struct. Biol.* **2004**, *14*, 757–764.
- [3] a) A. J. Skerra, *J. Mol. Recognit.* **2000**, *13*, 167–187; b) G. Folkers, C. D. P. Klein, *Angew. Chem. Int. Ed.* **2001**, *40*, 4175–4177–4305; *Angew. Chem.* **2001**, *113*, 4303–4305; c) C. Khosla, P. B. Har-bury, *Nature* **2001**, *409*, 247–252; d) T. C. Bruice, *Acc. Chem. Res.* **2002**, *35*, 139–148.
- [4] a) J. R. Moran, S. Karbach, D. J. Cram, *J. Am. Chem. Soc.* **1982**, *104*, 5826–5828; b) J. R. Moran, J. L. Ericson, E. Dalcanale, J. A. Bryant, C. B. Knobler, D. J. Cram, *J. Am. Chem. Soc.* **1991**, *113*, 5707–5714; c) D. J. Cram, J. M. Cram, *Container Molecules and Their Guests*, Royal Society of Chemistry, Cambridge, UK, **1994**, p. 85–130.
- [5] a) D. M. Rudkevich, J. Rebek Jr., *Eur. J. Org. Chem.* **1999**, 1991–2005; b) P. L. Wash, A. R. Renslo, J. Rebek Jr., *Angew. Chem. Int. Ed.* **2001**, *40*, 1221–1222; *Angew. Chem.* **2001**, *113*, 1261–1262; c) S. Xiao, D. Ajami, J. Rebek Jr., *Chem. Commun.* **2010**, *46*, 2459–2461; d) A. Lledo, J. Rebek Jr., *Chem. Commun.* **2010**, *46*, 1637–1639.
- [6] a) D. Ajami, L. Liu, J. Rebek Jr., *Chem. Soc. Rev.* **2015**, *44*, 490–499; b) D. Ajami, J. Rebek Jr., *Acc. Chem. Res.* **2013**, *46*, 990–999.
- [7] A. R. Renslo, J. Rebek Jr., *Angew. Chem. Int. Ed.* **2000**, *39*, 3281–3283; *Angew. Chem.* **2000**, *112*, 3419–3421.
- [8] a) B. W. Purse, P. Ballester, J. Rebek Jr., *J. Am. Chem. Soc.* **2003**, *125*, 14682–14683; b) J. Rebek Jr., *J. Org. Chem.* **2004**, *69*, 2651–2660; c) T. Iwasawa, R. J. Hooley, J. Rebek Jr., *Science* **2007**, *317*, 493–496.
- [9] a) Y. Inokuma, S. Yoshioka, M. Fujita, *Angew. Chem. Int. Ed.* **2010**, *49*, 5750–5752; b) T. Murase, Y. Nishijima, M. Fujita, *Chem. Asian J.* **2012**, *7*, 826–829.
- [10] M. D. Pluth, R. G. Bergman, K. N. Raymond, *Acc. Chem. Res.* **2009**, *42*, 1650–1659.
- [11] a) M. Guitet, P. Zhang, F. Marcelo, C. Tugny, J. Jimenez-Barbero, O. Buriez, C. Amatore, V. Mouries-Mansuy, J. P. Goddard, L. Fensterbank, Y. Zhang, S. Roland, M. Menand, M. Sollogoub, *Angew. Chem. Int. Ed.* **2013**, *52*, 7213–7218; b) M. Jouffroy, R. Gramage-Doria, D. Armspach, D. Semeril, W. Oberhauser, D. Matt, L. Toupet, *Angew. Chem. Int. Ed.* **2014**, *53*, 3937–3940.
- [12] T. Iwasawa, P. L. Wash, C. Gibson, J. Rebek Jr., *Tetrahedron* **2007**, *63*, 6506–6511.
- [13] C. Gibson, J. Rebek Jr., *Org. Lett.* **2002**, *4*, 1887–1890.
- [14] S. Shenoy, F. R. Pinacho Crisostomo, T. Iwasawa, J. Rebek Jr., *J. Am. Chem. Soc.* **2008**, *130*, 5658–5659.
- [15] a) Z. J. Wang, K. N. Clary, R. G. Bergman, K. N. Raymond, F. D. Toste, *Nature Chem.* **2013**, *5*, 100–103; b) M. Raynal, P. Ballester, A. Vidal-Ferran, P. W. N. M. van Leeuwen, *Chem. Soc. Rev.* **2014**, *43*, 1660–1733.
- [16] T. Iwasawa, Y. Nishimoto, K. Hama, T. Kamei, M. Nishiuchi, Y. Kawamura, *Tetrahedron Lett.* **2008**, *49*, 4758–4762. Phosphorus moieties of **1**, **4**, and **6** are not readily hydrolyzed with water because no decomposition was observed with the washing step in preparation.
- [17] K. Ohashi, K. Ito, T. Iwasawa, *Eur. J. Org. Chem.* **2014**, 1597–1601.

- [18] M. Kanaura, K. Ito, M. P. Schramm, D. Ajami, T. Iwasawa, *Tetrahedron Lett.* **2015**, *56*, 4824–4828.
- [19] a) J.-M. Lehn, *Supramolecular Chemistry: Concepts and Perspectives*; VCH, Weinheim, Germany, **1995**; b) J. W. Steed, J. L. Atwood, *Supramolecular Chemistry: An Introduction*, Wiley, Chichester, UK, **2000**.
- [20] The mechanism by which stereoselectivity occurs is not yet fully understood even though steric hindrance likely plays an important role, in this. For complex **3**, the supramolecular interactions between Au–Cl and quinoxaline-walls might stabilize the conformation of inward orientation.
- [21] M. Degardin, E. Busseron, D.-A. Kim, D. Ajami, J. Rebek Jr., *Chem. Commun.* **2012**, *48*, 11850–11852.
- [22] CCDC CCDC-1407998 (for **3**) contain(s) the supplementary crystallographic data for this paper. These data can be obtained free of charge from The Cambridge Crystallographic Data Centre. Triclinic, space group $P\bar{1}$, colorless, $a = 13.8433(6)$ Å, $b = 24.3818(10)$ Å, $c = 28.6654(5)$ Å, $\alpha = 74^\circ$, $\beta = 88^\circ$, $\gamma = 79^\circ$, $V = 9130(7)$ Å³, $Z = 4$, $T = 173$ K, $d_{\text{calcd.}} = 1.302$ g cm⁻³, $\mu(\text{Mo-K}\alpha) = 1.723$ mm⁻¹, $R_1 = 0.0644$, $wR_2 = 0.1894$, GOF = 1.027.
- [23] V. A. Azov, B. Jaun, F. Diederich, *Helv. Chim. Acta* **2004**, *87*, 449–462.
- [24] a) A. S. K. Hashmi, *Chem. Rev.* **2007**, *107*, 3180–3211; b) Z. Li, C. Brouwer, C. He, *Chem. Rev.* **2008**, *108*, 3239–3265; c) A. Arcadi, *Chem. Rev.* **2008**, *108*, 3266–3325.
- [25] a) N. Marion, R. S. Ramon, S. P. Nolan, *J. Am. Chem. Soc.* **2009**, *131*, 448–449; b) D. Wang, R. Cai, S. Sharma, J. Jirak, S. K. Thummanapelli, N. G. Akhmedov, H. Zhang, X. Liu, J. L. Peterson, S. Shi, *J. Am. Chem. Soc.* **2012**, *134*, 9012–9019; c) Y. Xu, X. Hu, J. Shao, G. Yang, Y. Wu, Z. Zhang, *Green Chem.* **2015**, *17*, 532–537.
- [26] In Figure 2 (b–d) and Figure S1 (d–e), the cavitand peaks almost disappear as a result of a mismatch with the NMR spectroscopic time scale. We think there are two reasons for this. One is the slow equilibrium between vase and kite conformers because the bulky substrate forces the kite formation. For make sure, we tried a low-temperature NMR experiment; however, we were unable to record data because of the low solubility of its complex. The second reason is a typical pi interaction between Au⁺ and alkyne that caused peaks broadening, which has been observation previously in ref.^[27].
- [27] M. T. Reetz, K. Sommer, *Eur. J. Org. Chem.* **2003**, 3485–3496.
- [28] Results of up- and downfield portion of the ¹H NMR spectra are listed in Figure S1, see Supporting Information.
- [29] The MS spectrum is contained in the Supporting Information.
- [30] T. Zdobinsky, P. S. Maiti, R. Klajn, *J. Am. Chem. Soc.* **2014**, *136*, 2711–2714.
- [31] a) J. J. K.-Smith, S. T. Staben, F. D. Toste, *J. Am. Chem. Soc.* **2004**, *126*, 4526–4527; b) A. Ochida, H. Ito, M. Sawamura, *J. Am. Chem. Soc.* **2006**, *128*, 16486–16487.
- [32] The effect of conventional phosphorus ligands, such as PPh₃, P(OPh)₃ and other bulky phosphines, was reported in ref.^[24,25,27,31].

Received: November 11, 2015

Published Online: December 15, 2015